WEP Warwick Evans Publishing

International Journal of Mechanical and Electrical Engineering

ISSN: 3005-9615 (Print), ISSN: 3005-7132 (Online) | Volume 5, Number 2, Year 2025
DOI: https://doi.org/10.62051/ijmee.v5n2.06
Journal homepage: https://wepub.org/index.php/IJMEE/index

Experimental Study on Liquid-assisted Nanosecond Laser Processing of Inconel 718 Micropores

Xuri Li [1, 2, 3], Shufeng Sun [1, 2, 3, *], Pingping Wang [2, 3], Fengyun Zhang [1, 2, 3], Jin Wang [1, 2, 3], Tao Wei [1, 2, 3], Gongliang Chen [1, 2, 3], Junbao Li [1, 2, 3], Yong Zhu [1, 2, 3]

[1] Discipline Innovation and Wisdom Introduction Base of High-end Laser Intelligent Manufacturing Technology and Equipment (No. D21017), Qingdao University of Technology, Qingdao 266525, China

[2] Shandong Provincial Key Laboratory of Laser Green Intelligent Manufacturing Technology, Qingdao University of Technology, Qingdao. 266525, China

[3] Qingdao University of Technology, Qingdao. 266525, China

* Corresponding Author: Shufeng Sun (Email: sunshufeng@qut.edu.cn)

ABSTRACT

In this paper, the experiment of IN718 superalloy was carried out with the aid of liquid, and the influence of liquid aid on key indexes such as hole taper and diameter of inlet and outlet was systematically analyzed. At the same time, the chemical element composition of the hole wall was detected, and the thickness of oxide layer formed in different environments during machining was studied. Finally, the processing mechanism of IN718 superalloy nanosecond laser drilling under liquid-assisted conditions is discussed. The results show that both water-assisted and liquid-assisted can improve the quality of micropores in different degrees compared with the condition without auxiliary field in air, especially the effect of liquid-assisted is the most significant. Under this condition, the hole taper is reduced by 67%. In addition, with the help of liquid, the content of oxygen element in the pore wall of micropores is greatly reduced, and the element composition is closer to the base material. This study provides important theoretical support and technical optimization direction for nanosecond laser drilling technology.

KEYWORDS

Nanosecond Laser; Chemical Liquid; Inconel 718; Plasma; Superalloy.

1. INTRODUCTION

With the development of aerospace technology, the requirements for turbine blade gas film holes are constantly increasing [1]. At present, in addition to traditional processing methods, the micro-hole processing methods also rely on unconventional processing methods in many cases, including mechanical processing [2], electric discharge machining [3], electrochemical processing [4] and laser processing [5]. Among these methods, laser processing has become the main way of microhole processing because of its high efficiency, economy, quality and other advantages.

In order to solve the negative effects of heat affected zone, recast layer and micro-crack in laser processing, liquid assisted laser processing has come into everyone's vision. Marimuthu et al. [6] found that water jet assisted laser drilling can effectively promote melt discharge from the hole through the cold ablation effect of water flow, avoid melt residue phenomenon and increase the drilling rate, and significantly improve the hole quality of metal matrix composite materials (such as silicon carbide particles reinforced aluminum MMC). Li et al. [7] proposed a two-step coaxial water

jet assisted composite laser drilling (TS-CWALD) method. By optimizing parameters through regression model and response surface method, the inlet diameter, outlet diameter and hole taper were successfully optimized to achieve low HAZ and high precision machining. Ren et al. [8] showed that at a low pulse repetition rate (such as 25 kHz), using underwater assisted drilling could reduce the hole cone Angle by 64.19% (about 4.20°), increase the hole cross-sectional area by 46%, and significantly reduce the residual debris and ablations on the hole side wall. On aluminum blocks and SIC samples, Krstulovi et al. [9] found by adjusting the thickness of the water layer that when the thickness of the water layer reached about 3 mm, the laser ablation effect of the aluminum target was the best - the volume and depth of the crater were 28 and 18 times higher than that in the air environment, respectively, and the redeposition was avoided at the same time. Laakso et al. [10] used ultra-short pulse laser assisted by back-water to process high-quality micropores on silicon, removing debris on the pore wall and reducing the deformation of micropores. For titanium materials and metal filter processing, Mendiratta et al. [11] found that coating thin water layer on the back of titanium workpiece can significantly reduce the heat-affected zone and hole taper, and obtain microholes with almost no taper. Zhang et al. [12] used back-water assisted laser processing on stainless steel to reduce the taper of the hole and improve the roundness and consistency of the hole.

In order to further optimize the quality of microholes on the basis of water assistance, a method of chemical liquid-assisted nanosecond laser microhole machining is proposed. Wang et al. [13] proposed an in-situ machining method using environmentally friendly chemical liquid to eliminate the defect layer through chemical etching at local high temperature, and restricted the expansion of high-temperature gas and plasma by liquid confinement effect, so that the laser plasma ablation pressure acted more directly on the substrate, thus optimizing the pore shape and surface roughness. At the same time, Li et al. [14] proposed the thermochemical mechanism of contact between electron beam and material interaction point by using environmentally friendly salt solution, which significantly improved the removal efficiency of 316 stainless steel workpiece, and at the same time removed the recast layer in processing, and the material removal rate increased by 300% compared with traditional laser processing.

2. EXPERIMENTAL PROCEDURE

2.1. Materials

In this study, IN718 superalloy with a thickness of 1± 0.01mm was selected as the experimental sample, and its chemical composition was shown in Table 1. Nickel-based superalloys are known for their excellent corrosion resistance, mainly due to their high proportion of nickel content. Nickel has a high electrode potential and excellent surface passivation ability, which can effectively resist the erosion of halogen gases and alkaline solutions, showing excellent stability. In addition, Cr, Mo and other elements in the alloy have good solid solution ability in the nickel matrix, and show strong corrosion resistance to a variety of media. The synergistic action of many elements gives nickel-based superalloys unique corrosion resistance properties, making them a key specialty material.

Table 1. Chemical composition of IN718

element	Ni	Cr	Fe	Nb	Mo	Ti	Co	Cu	Si	Mn	C
Take up a proportion of/%	53.66	18.41	17.9	4.92	2.87	0.96	0.34	0.13	0.09	0.08	0.03

2.2. Experimental Design

Before the start of the experiment, the surface of IN718 superalloy was polished with a grinder to obtain a smooth and flat surface. Then, using anhydrous ethanol as cleaning agent, the samples were thoroughly cleaned in the ultrasonic cleaning machine and put into the experiment.

In the experiment, the back liquid assisted method was used to make the liquid cover the lower surface of the workpiece without touching the upper surface, so as to avoid the adverse effects of the liquid weakening the laser energy or causing laser refraction. At the beginning of the experiment, the liquid had little influence on the processing. However, when the through hole is formed, the chemical liquid enters the microhole, which has a significant impact on the subsequent processing.

The whole process of laser processing is carried out by scanning and filling. Each layer consists of multiple concentric circles with the same radius difference between them. The maximum concentric circle diameter is 400 μm, the minimum is 20 μm, and the diameter difference between adjacent circles is 40 μm. The processing sequence is circular processing from outside to inside.

After the experiment, in order to obtain the cross section of the hole, grinding and polishing were used, and the distribution of the recast layer was observed by corrosion experiment. Then, the entrance, exit and cross section morphology of the hole were photographed by laser confocal scanning microscope, and the appearance of the hole side wall was further photographed and analyzed, and the surface roughness of the hole side wall was measured by microscope analysis software

3. WATER ASSISTED NANOSECOND LASER MICROHOLE MACHINING

3.1. The Influence of Liquid Assisted and Different Liquid Layer Thickness on Micropore Morphology and Size

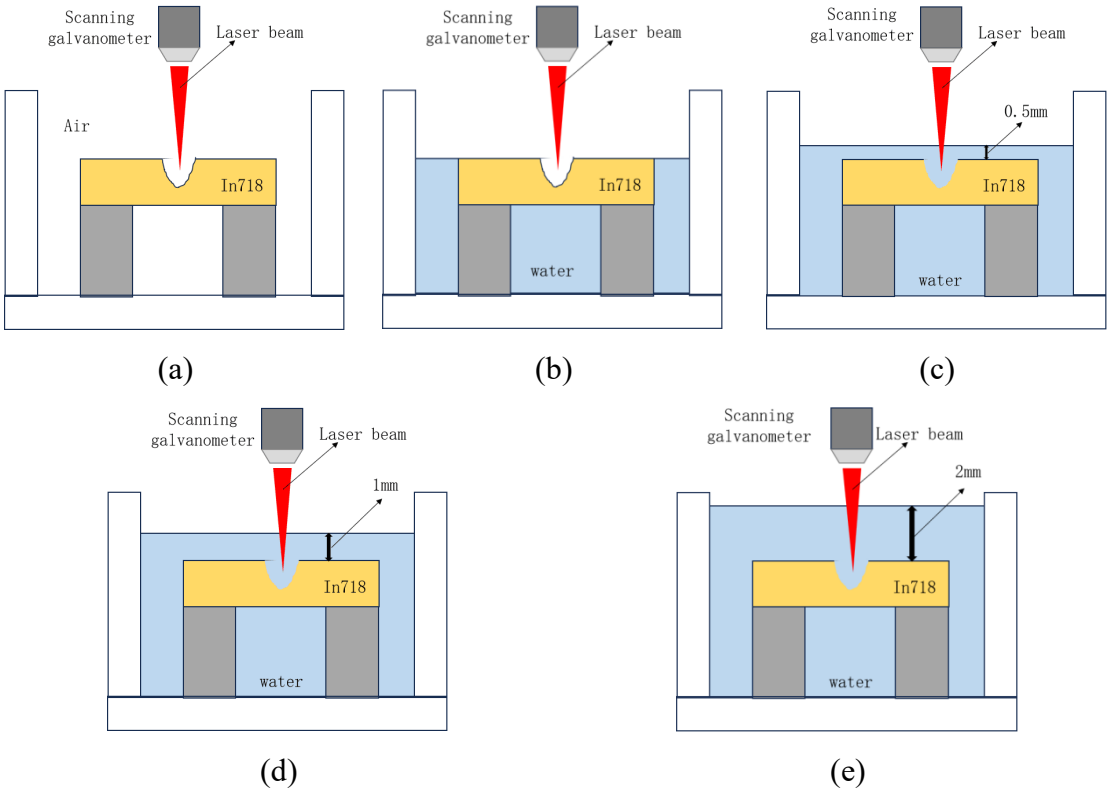

Figure 1. Diagram of water-assisted nanosecond laser microhole machining without liquid and with different thickness of liquid layer. (a) liquidless (b) 0mm (c) 0.5mm (d) 1mm (e) 2mm

The diagram of water-assisted nanosecond laser microhole machining without liquid assistance and with different liquid layer thickness is shown in Figure 1, where the liquid layer thickness refers to the height of the liquid layer surface over the upper surface of the material during the processing. Considering that in the laser processing process, different liquid layer thickness will lead to different

absorption, refraction and scattering effects of water on laser, and different liquid layer thickness will lead to different cooling effects of microholes during the processing process, the liquid layer thickness plays a key role in the processing quality and size of microholes in the water-assisted laser processing microhole experiment. The experiments were carried out by water-assisted machining without liquid and with liquid layer thickness of 0mm, 0.5mm, 1mm and 2mm respectively.

As can be seen from Figure 2, when there is no liquid assistance, there is an obvious heat-affected zone around the inlet and outlet of the micropore, and there is recast accumulation around the orifice. It can be seen from the micropore topography of water-assisted machining under different liquid layers thickness that there is a metallic luster area around the entrance of the micropore of water-assisted machining, which is actually a micropit formed by partial ablation of laser energy and cavitation rupture through scattering and refraction. There is also a black area around the metallic luster area, which is the heat affected zone generated during the microhole machining process. With the increase of liquid layer thickness, the area of metal gloss area gradually expands, and the heat affected zone around the orifice also increases. The reason for this phenomenon is that the increase in the thickness of the liquid layer enhances the refraction and scattering effect of water on the laser, increases the area of the laser, increases the number of bubbles generated by the water absorbing laser energy, and increases the micropores caused by the shock wave caused by the collapse of the bubble. In addition, the volume of the plasma in the liquid is smaller than in the air, and the heat exchange between the high-density plasma and the surface of the material is more significant under water, resulting in the expansion of the ablation area. With the increase of water layer thickness, the plasma density further increases, and the ablation area also expands.

At the same time, the liquid absorbs the laser energy and forms tiny bubbles inside. When these bubbles move to the junction of liquid and air, due to the pressure difference between the liquid and air, the bubbles will burst and produce high-speed microjets, forming an impact on the surface of the workpiece, and then forming micro-pits. With the increase of the thickness of the water layer, the amount of water vaporization increases, the number of microbubbles also increases, and the impact force of the microjet is enhanced, resulting in a more obvious micro-pit phenomenon at the orifice.

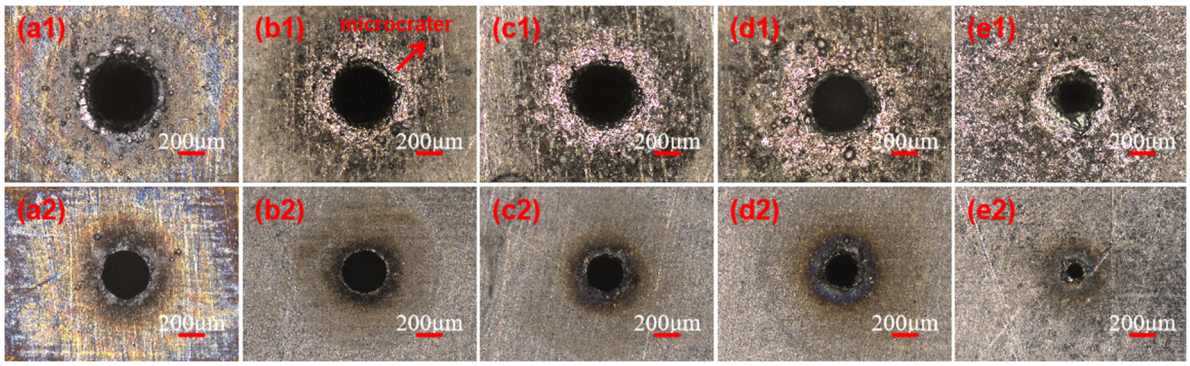

Figure 2. Inlet and outlet morphologies of micropores processed in water-assisted environment with different liquid layer thicknesses (1) Inlet (2) Outlet (a) 0mm (b) 0.5mm (c) 1mm (d) 2mm

As can be seen from FIG.3 (a), when no liquid is assisted, the inlet diameter of the microhole is the largest, and the inlet diameter is 470.383μm and the outlet diameter is 380.612μm, but the inlet diameter of the microhole is far beyond the preset inlet diameter. Under the water-assisted condition, with the increase of liquid layer thickness, the inlet diameter of micropores first increased and then decreased. When the liquid layer thickness was 0mm, the inlet diameter of micropores was 426.839μm, and when the liquid layer thickness increased to 0.5mm, the inlet diameter of micropores reached the maximum 442.547μm, and then the inlet diameter of micropores continued to decrease with the increase of liquid layer thickness. When the liquid layer thickness is 2mm, the minimum is 271.328μm. The outlet diameter of the micropore decreases with the increase of the liquid layer

thickness. When the liquid layer thickness is 0mm, the outlet diameter of the micropore is 355.813μm at the maximum. With the increase of the liquid layer thickness, the inlet diameter of the micropore decreases with the increase of the liquid layer thickness, and the outlet diameter of the micropore is 68.736μm when the liquid layer thickness is 2mm. This is because the water has the absorption, scattering and refraction of the laser, when the liquid layer thickness increases, the absorption, scattering and refraction of the water on the laser is enhanced, so that the laser energy is reduced, and the scope of action of the laser on the surface of the material is increased, which leads to the increase of the inlet diameter of the microhole and the decrease of the outlet diameter. As the liquid layer thickness continues to increase, too large liquid layer thickness will lead to a significant weakening of laser energy, resulting in a decrease in the diameter of the micropore inlet and outlet.

As can be seen from Figure 3(b), when there is no liquid assistance, the inlet roundness of the microhole is 0.971, which is the best inlet roundness, but the taper of the microhole is not the best 5.14°. When the liquid layer thickness is 0mm, the circularity of the microhole entrance is the highest of 0.965, and with the increase of the liquid layer thickness, the circularity of the microhole entrance decreases, and when the liquid layer thickness is 2mm, the circularity of the microhole entrance is only 0.939. This is because when the thickness of the liquid layer increases, the refraction and scattering effect of water on the laser is enhanced, resulting in a decrease in the roundness of the micropore entrance. When the liquid layer thickness is 0mm, the minimum taper of the microhole is 4.068°. With the increase of the liquid layer thickness, the taper of the microhole increases sharply. When the liquid layer thickness increases to 2mm, the taper of the microhole increases to 11.568°.

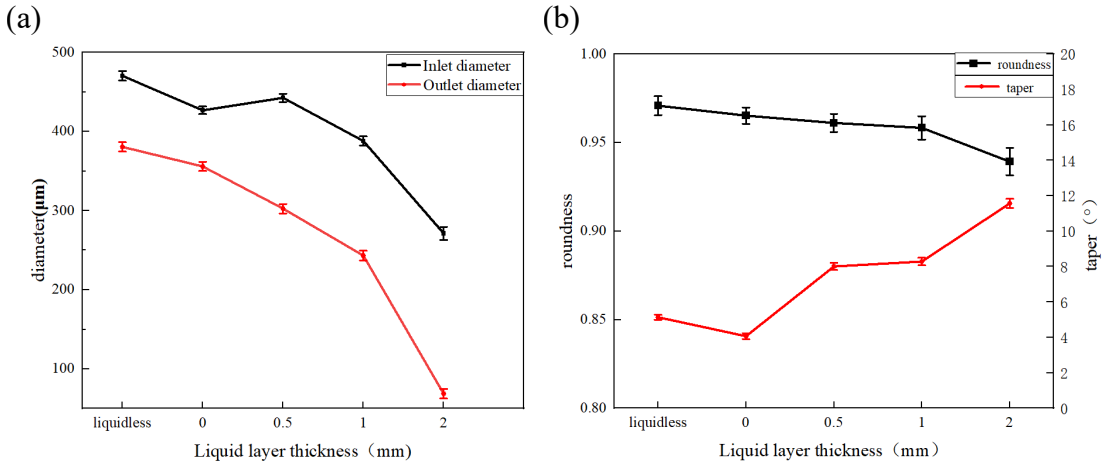

Figure 3. The micropore size of water assisted processing without liquid and with different thickness of liquid layer (a) Inlet diameter, outlet diameter (b) Roundness, taper

The experimental results of water-assisted nanosecond laser microhole machining without liquid assistance and under different liquid layer thickens show that when the water-assisted liquid layer thickness is 0mm, the ablation zone and heat-affected zone of the microhole are smaller, the taper of the microhole is the smallest, the inlet circularity of the microhole is slightly worse than that without liquid assistance, and the comprehensive microhole quality is the highest. The inlet diameter of the microhole is 426.839μm, the outlet diameter is 355.813μm, the inlet roundness is 0.965, and the taper is 4.068°.

3.2. Mechanism Analysis of Back-Water Assisted Laser Microhole Machining

The water-assisted micropore processing method with a liquid layer thickness of 0mm is called the back-water assisted method. The principle diagram of back-water assisted nanosecond laser drilling is shown in Figure 4. FIG. 4 (a) shows the blind hole stage, in which water has little influence on laser processing of microholes. Before the through hole is formed, water cannot enter the hole and directly participate in the process of microhole processing. Therefore, in the blind hole stage, the

influence of water on microhole processing is small. At the same time, the plasma generated during this stage of processing has a shielding effect on the laser, and the refraction of the plasma on the laser causes the actual focus position of the laser to drop, which has an impact on the processing effect.

The through hole stage is shown in Figure 4 (b). At this time, a through hole has been formed. After water enters the hole through the outlet of the microhole under pressure, it absorbs laser energy and quickly vaporizes, producing bubbles. When the bubble collapses, the micro shock wave can enhance the local force of the laser, and this impact effect can effectively promote the removal of the hole wall, so as to improve the processing efficiency. In addition, the bubbles generated by vaporization promote the flow of water during the rising process, and the water flow drives the ablative materials and debris generated in the processing, reducing their adhesion on the hole wall, so that the laser can more directly act on the matrix material in the hole. When the bubbles without collapse rise to the entrance of the microhole, part of the bubbles enter the water film, rupture and generate shock wave under the influence of pressure difference, forming the affected area of bubble rupture. The impact force of rupture will produce the microhole area with metallic luster at the orifice, as shown in Figure 2. At the same time, the pressure forming the water limits the expansion of the plasma, which makes the blowback pressure generated when the plasma expands in the water greater, which helps to push the molten material away from the surface of the hole wall and out of the hole, thereby preventing it from re-solidifying on the surface of the workpiece to form a recast layer. At the same time, water can also reduce the size and duration of the plasma, so that the shielding effect of the plasma on the laser is reduced.

As shown in Figure 4 (c), the microhole processing is completed, at which time the laser stops processing, and the bubble and plasma disappear.

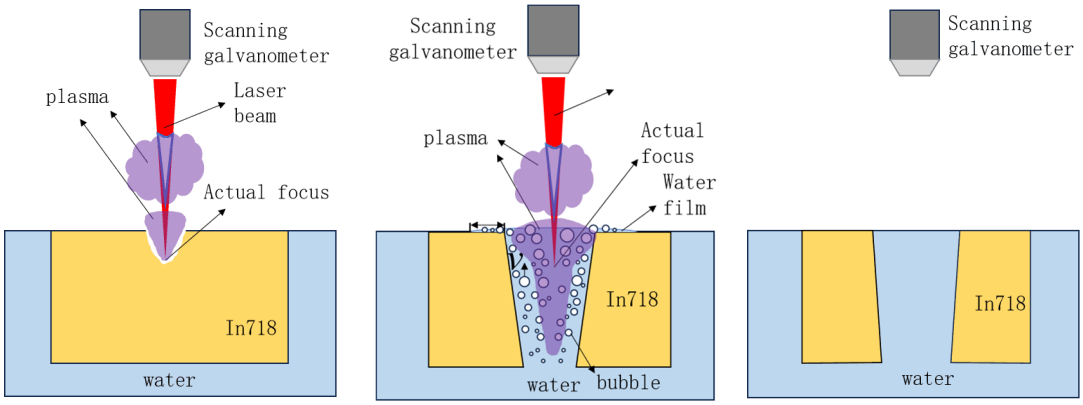

Figure 4. Back water assisted nanosecond laser drilling schematic (a) Blind stage; (b) Through-hole stage; (c) Completion phase

4. CHEMICAL LIQUID ASSISTED NANOSECOND LASER MICROHOLE MACHINING

4.1. Selection of Chemical Solution

When selecting a chemical liquid, it should be ensured that it does not react with the substrate at room temperature, and it can effectively promote material removal under the high temperature conditions of laser processing, thereby improving the quality of the micropores. For the composition of IN718 nickel-based superalloy, it is necessary to select a suitable chemical solution. The main components of the alloy are shown in Table 1.

IN718 nickel-based superalloy has excellent corrosion resistance, mainly due to the high electrode potential of its main component nickel and strong surface passivation ability, making it resistant to halogen gas and alkaline solution erosion, maintaining a high degree of stability. In addition, chromium (Cr), molybdenum (Mo) and other elements in nickel solid solution ability is good, and has corrosion resistance to a variety of media, these factors work together to make nickel-based superalloy become a special corrosion resistant material. The following is a detailed analysis of the properties of each element:

Nickel (Ni) : Electrode potential is -0.25V. At normal temperature, the dense oxide film formed on the surface of nickel can not only prevent the oxidation of the internal material, but also resist the erosion of alkaline solution. Nickel slowly dissolves in dilute acids (such as dilute hydrochloric acid, dilute sulfuric acid, dilute nitric acid) to produce hydrogen and green Ni2+. Nickel does not react with oxidants, but can react with halogens when heated.

Chromium (Cr) : The electrode potential is -0.74V, has a strong passivation ability, and is stable to oxygen and moisture at room temperature. Once the passivation film is destroyed, chromium rapidly reacts with dilute hydrochloric acid to form chloride salts and hydrogen. At high temperatures, chromium forms Cr2O3, giving it resistance to oxidation and corrosion. In addition, chromium can react directly with halogens, carbon and nitrogen at high temperatures.

Iron (Fe) : with high electronegativity and covalent single electron structure, it is easy to oxidize in air to form iron oxide. At room temperature, iron can continue to react with dilute acids, but concentrated acids will passivate its surface and prevent further reactions. Iron is burned in oxygen to form Fe3O4, which can react with halogens, carbon and phosphorus when heated.

Niobium (Nb) : As a transition metal, it does not react with oxygen, acid, and base at room temperature, but can react at high temperatures. Molybdenum (Mo) at room temperature does not react with air, hydrochloric acid, dilute nitric acid, dilute sulfuric acid and alkaline solution, only soluble in concentrated nitric acid, concentrated sulfuric acid and boiled hydrochloric acid.

Titanium, cobalt, copper, silicon, manganese, carbon and other elements are low in content, not detailed here.

In summary, the main components of Inconel718, nickel, chromium and iron, can react with dilute acids and halogens. At room temperature, these metals form a protective oxide film in an oxidizing solution, and the oxide film decomposes at high temperatures. Therefore, the selected chemical solution should be acidic and oxidizing, protect the surface of the material at room temperature, and promote the removal of the material at high temperature. Based on laboratory conditions, hydrochloric acid solution and sodium nitrate solution are recommended. Hydrochloric acid provides an acidic environment and halogens that aid in material removal, while sodium nitrate provides an oxidizing environment.

4.2. The Ratio of Chemical Liquid Concentration

In the determined mixture of hydrochloric acid and sodium nitrate, HCl is fully ionized to H+ and Cl-, and NaNO3 is ionized to Na+ and NO3-. H+ provides an acidic environment, Cl- accelerates the reaction through halogen properties, while NO3- is oxidizing under acidic conditions.

At 25℃ and 90℃, 10mm×10mm×1mm Inconel718 nickel-based alloy materials were immersed in different concentrations of hydrochloric acid-sodium nitrate mixed solutions. Before and after soaking, the appropriate concentration ratio of chemical liquid is selected by weighing the material weight loss. At 25℃, the material was soaked for 20 minutes, then removed, cleaned with alcohol and weighed. The material was also soaked for 20 minutes at 90 ° C, then cleaned and weighed.

The concentration of pure hydrochloric acid solution used in the experiment is 36%~38%. In order to facilitate calculation, the mass fraction of the solution needs to be converted into molar concentration, and the conversion formula is as follows: (1):

$$C = 1000 \times \rho \times W / M \tag{1}$$

Where, ρ is the density of the solution, W is the mass fraction of the solution, M is the molar mass of the solution, and C is the molar concentration of the solution, which is about 12mol/L after conversion. Using the molar concentration, the corresponding volume of the solution can be calculated as equation (2):

$$C_1 V_1 = C_2 V_2 \tag{2}$$

Where C1 is the molar concentration of the solution before configuration, V1 is the volume of the solution before configuration, C2 is the molar concentration of the solution to be configured, and V2 is the volume of the solution to be configured.

The concentration of NaNO3 solution used in the experiment was 4mol/L. The experiment shows that when the concentration of HCl exceeds 3mol/L, the solution appears green and the surface of the material begins to corrode, which cannot meet the requirements of chemical liquid selection. With the increase of HCl concentration, the acidity and oxidation of the solution are enhanced, and the corrosion effect is intensified. Therefore, 1mol/L and 2mol/L HCl solutions and 1mol/L to 4mol/L NaNO3 solutions were selected for experiments, and the results were shown in Figure 5.

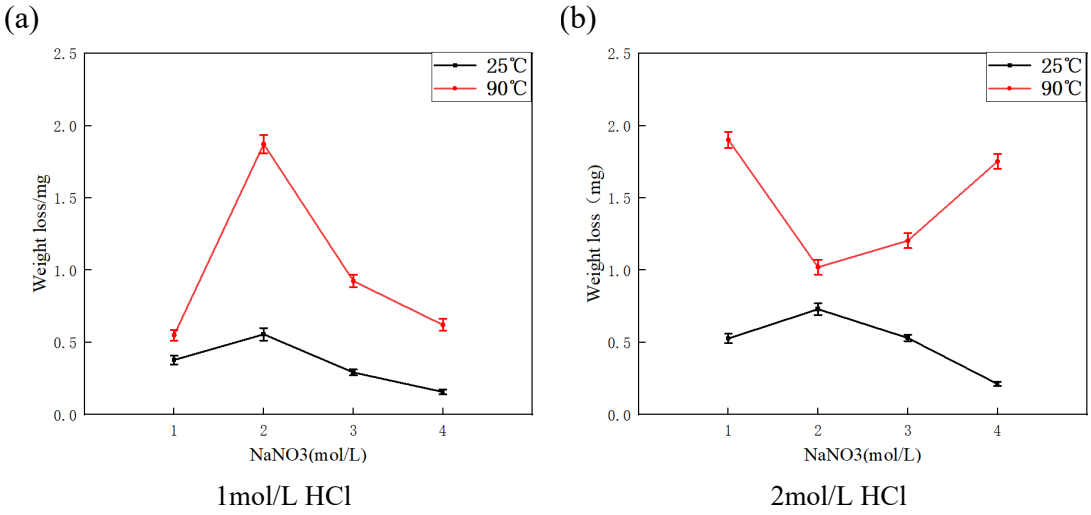

Figure 5. Weight loss of materials in different concentrations of chemical liquids

FIG. 5 (a) shows that when the concentration of HCl is 1mol/L, the weight loss of the material increases when the concentration of NaNO3 increases from 1mol/L to 2mol/L. The weight loss decreased when the concentration increased from 2mol/L to 4mol/L, and the maximum weight loss occurred at 2mol/L NaNO3 concentration. This is because when the concentration of NaNO3 is less than 2mol/L, the oxidation of the solution is enhanced, but it is not enough to passivate the material, thus increasing the dissolution amount. When the concentration of NaNO3 exceeds 2mol/L, the excessive oxidation results in the passivation of the material surface, which inhibits the subsequent reaction.

FIG. 5 (b) shows that when the concentration of HCl is 2mol/L, the trend at 20°C is similar to that at 1mol/L, while when the concentration of NaNO3 rises from 1mol/L to 2mol/L at 90°C, the weight loss of the material decreases and begins to increase after exceeding 2mol/L. With the increase of HCl concentration, the concentration of H+ in the solution increases, and the activity of NO3-

increases with the increase of temperature. Therefore, the weight loss of the material at 90℃ is positively correlated with the concentration of NaNO3.

Therefore, when the concentration of HCl is 2mol/L and the concentration of NaNO3 is 4mol/L, the weight loss is less and the reaction is slow at room temperature. The weight loss at high temperature is larger, the reaction is faster, and it meets the selection criteria of chemical liquid.

4.3. Effect of Chemical Liquid Layer Thickness on Micropore Morphology and Size

In the experiment, hydrochloric acid solution and sodium nitrate solution were used as chemical solutions. Considering the different thickness of liquid layer during micropore machining and the different degree of participation of chemical solution in the micropore machining process, the auxiliary methods of chemical solution with liquid layer thickness of 0mm, 0.5mm, 1mm and 2mm were used respectively in the experiment, as shown in Figure 6.

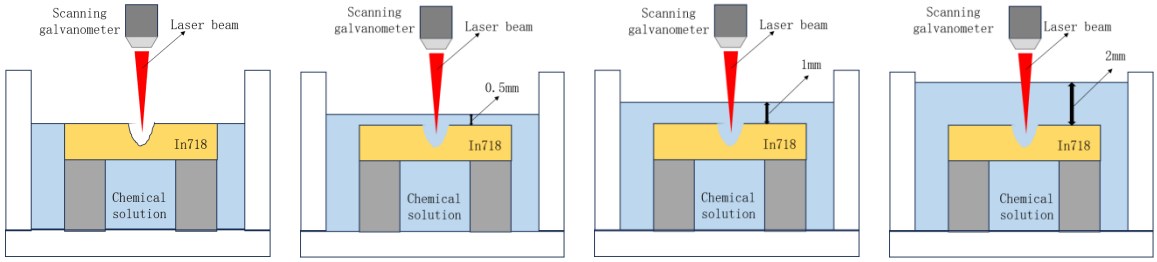

Figure 6. Schematic diagram of chemical solution-assisted nanosecond laser microhole machining under different thickness of liquid layer. (a) 0mm (b) 0.5mm (c) 1mm (d) 2mm

It can be seen from the micropore topography of chemical liquid-assisted machining under different liquid layer thickths in FIG. 7 that different from water-assisted micropore machining, only when the liquid layer thickness is 0mm, there is a small range of metallic luster area around the micropore inlet of chemical liquid-assisted machining. This is because when the thickness of the liquid layer is 0mm, the chemical liquid only comes into contact with the micropore inlet after forming a small amount of through holes, so the chemical reaction of the chemical liquid to the micropit around the micropore inlet is not strong. When the thickness of the liquid layer exceeds 0mm, the full name of the chemical liquid participates in the whole process of micropore processing, so that part of the micro-pit formed by the laser energy ablation and cavitation rupture through scattering and refraction reacts with the chemical liquid in a high temperature environment, greatly reducing the micro-pit. In addition, compared with the micropore topography of the chemical liquid-assisted processing (FIG. 7) and that of the water-assisted processing (FIG. 2), the micro-pore outlet recast produced by the chemical liquid-assisted processing is significantly reduced, because the chemical liquid reacts with the material at high temperature during the laser processing process and removes the recast.

As shown in FIG. 8 (a), when micropores are processed in chemical fluids with different liquid layer thickths, the inlet diameter of micropores first increases and then decreases. When the liquid layer thickness is 0mm, the inlet diameter of micropores is 433.251μm; when the liquid layer thickness is increased to 0.5mm, the inlet diameter of micropores reaches the maximum of 468.674μm; when the liquid layer thickness continues to increase, the inlet diameter of micropores reaches the maximum of 468.674μm. When the liquid layer thickness reaches 2mm, the inlet diameter of the micropore reaches the minimum of 408.92μm, and the inlet diameter of the micropore decreases slightly. Compared with the inlet diameter of the microhole processed with the liquid layer thickness of 2mm (Figure 3), the inlet diameter of the microhole processed with the chemical liquid was significantly larger. This is because when the thickness of the chemical liquid layer is 0mm, the chemical liquid does not directly participate in the microhole machining process in the blind hole stage, so it does not

affect the microhole entrance size in the blind hole stage. However, when the thickness of the chemical liquid layer exceeds 0mm, the chemical liquid directly participates in the microhole machining process in the blind hole stage, and the removal of the material by the chemical liquid under high temperature environment leads to the increase of the diameter of the microhole entrance. The outlet diameter of micropores reaches a maximum of 371.732μm when the liquid layer thickness is 0mm, and decreases with the increase of the liquid layer thickness. The outlet diameter of micropores reaches a minimum of 102.736μm when the liquid layer thickness is 2mm. The reason is similar to that in the water processing of micropores, but when the chemical liquid is used to assist, because the chemical liquid helps to remove the material in a high temperature environment, the exit and entrance of the micropores are increased to different degrees compared with the water assisted process.

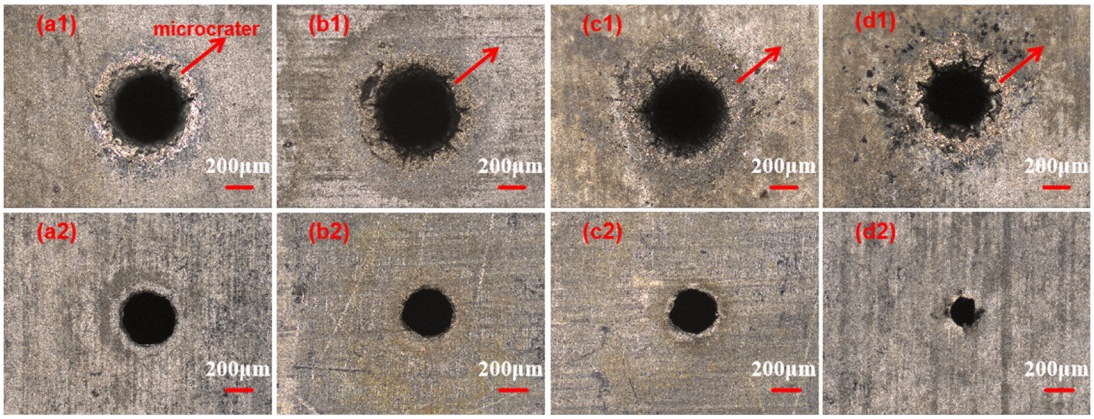

Figure 7. Inlet and outlet morphologies of micropores processed in chemical liquid-assisted environment with different liquid layer thicknesses (1) Inlet (2) Outlet (a) 0mm (b) 0.5mm (c) 1mm (d) 2mm

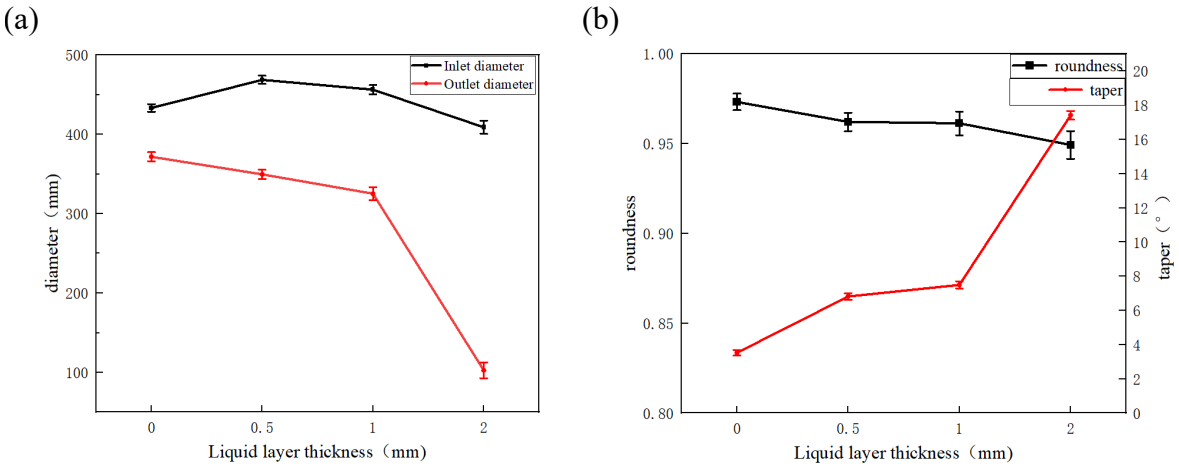

Figure 8. Micropore sizes processed in chemical liquid-assisted environments at different liquid layer thicknesses (a) Inlet diameter, outlet diameter (b) Roundness, taper

As shown in FIG. 8 (b), when the thickness of the chemical liquid layer is 0mm, the roundness of the micropore inlet is up to 0.968; with the increase of the liquid layer thickness, the roundness of the micropore inlet decreases to 0.949 when the thickness of the liquid layer is 2mm. This is because the refraction and scattering effect of the chemical liquid on the laser is enhanced when the thickness of the chemical liquid layer is increased. The roundness of the entrance of the microhole decreases. When the liquid layer thickness is 0mm, the minimum taper of the microhole is 3.524°. With the

increase of the liquid layer thickness, the taper of the microhole increases sharply. When the liquid layer thickness increases to 2mm, the taper of the microhole increases to 17.408°.

The experimental results of chemical liquid-assisted nanosecond laser microhole machining under different liquid layer thickness show that when the thickness of chemical liquid-assisted liquid layer is 0mm, the obtained microhole ablation zone and heat affected zone are smaller, the inlet circularity of microhole is the highest, the taper of microhole is the smallest, and the quality of microholes is the highest. The inlet diameter of the microhole is 433.251μm, the outlet diameter is 371.732μm, the inlet roundness is 0.973, and the taper is 3.524°.

4.4. Analysis of Mechanism of Laser Microhole Machining Aided by Chemical Solution

The chemical liquid-assisted microhole processing method with a liquid layer thickness of 0mm is called the back chemical liquid-assisted method. The principle diagram of back chemical liquid-assisted nanosecond laser drilling is shown in Figure 9. FIG. 9 (a) shows the blind hole stage, in which the chemical solution still cannot directly participate in the laser processing process. It can only play an indirect cooling effect, and the cooling effect is not obvious. Therefore, in the blind hole stage, the chemical solution has little influence on the microhole processing. In the normal temperature environment, the chemical liquid and the bottom and side materials have a weak chemical reaction to produce part of NO gas, resulting in a small number of bubbles. At the same time, the plasma generated during this stage of processing has a shielding effect on the laser, and the refraction of the plasma on the laser causes the actual focus position of the laser to drop, affecting the processing effect.

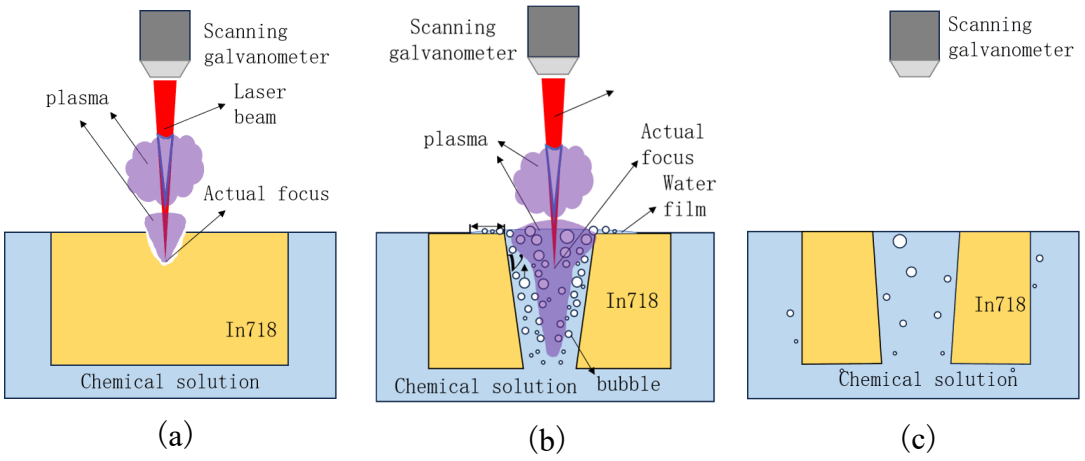

Figure 9. Back chemical liquid assisted nanosecond laser drilling schematic (a) Blind stage; (b) Through-hole stage; (c) Completion phase

Proceed to the through hole stage as shown in Figure 9 (b). At this time, through hole has been formed, and chemical liquid enters the hole through the micro-hole outlet under pressure. The chemical liquid assist will also produce the effect of bubble collapse to promote material removal, bubble rise to promote water flow to discharge ablative materials and debris, increase the recoil pressure generated by plasma to reduce the recast layer, reduce the size and duration of plasma to reduce the shielding effect on laser. In addition, in the high temperature environment of laser processing, the chemical liquid reacts violently with the material, and the chemical liquid mainly reacts with the main materials such as Ni, Cr, Fe and Nb in the Inconel 718 material. It reacts with the main element Ni to produce sodium chloride, nickel nitrate and hydrogen.

The high temperature environment of laser processing promotes the chemical reaction between the chemical liquid and the material, improves the removal effect of the material, and increases the inlet

diameter and outlet diameter of the microhole. In addition, due to the reaction between chemical liquid and material at high temperature, gas is produced, and the solubility of gas in water is low, so the production of gas increases the number of bubbles in water, improves the effect of bubble rise and water flow to discharge ablative materials and debris, and improves the material removal rate.

As shown in Figure 9 (c), when the microhole processing is completed, the laser stops processing and the plasma disappears. However, the waste heat generated in the laser processing process still promotes the chemical reaction between the chemical liquid and the material to remove the material, resulting in a small amount of gas and the formation of bubbles.

5. CONCLUSION

In this paper, the process optimization and mechanism of micropore preparation on Inconel 718 material by liquid-assisted (water and chemical solution) nanosecond laser processing technology are systematically studied.

First of all, unassisted laser microhole machining results in obvious microhole heat affected zone (HAZ) with a microhole taper of 5.14°, but a relatively high microhole entrance circularity of 0.971. Then, through water-assisted experiments, the effect of liquid layer thickness on micropore morphology was revealed. It was determined that the micropore quality was the best when the liquid layer thickness was 0mm (water-assisted), and the inlet circularity was 0.965 and the taper was 4.068°. The effects of bubble collapse, plasma confinement effect and melt scouring mechanism on the quality of micropores were also discussed.

In the chemical liquid-assisted processing, a mixed solution of HCL and sodium nitrate was selected combined with material composition analysis. On this basis, Inconel718 nickel-based alloy materials were immersed in HCL and sodium nitrate mixed solutions of different concentrations at room temperature and high temperature respectively to measure material weight loss. Determine the appropriate mixture of HCl and sodium nitrate (2 mol/L HCL and 4 mol/L $NaNO_3$). Subsequently, the optimal chemical liquid layer thickness (0mm) was determined through experimental optimization, and the recast layer was significantly reduced through the high-temperature chemical reaction mechanism, and the taper of the micropores was reduced. Under these conditions, microholes with entrance roundness of 0.973 and taper of 3.524° are machined. The experiments show that the liquid assisted machining can effectively reduce the taper of microholes, improve the dimensional accuracy and surface integrity through dynamic cooling, chemical collaborative etching and bubble impact effect, and provide theoretical and technological support for efficient precision machining of microholes in complex environments.

By comparing without auxiliary field, water assisted and chemical liquid assisted, it is found that without auxiliary field, the microhole taper and heat affected zone are larger, and the appearance of microhole inlet and outlet is poorer. When water is used, the taper of the microhole and the heat affected zone decrease, but the roundness of the entrance decreases. When chemical liquid is used, the heat affected zone, taper and orifice morphology of micropores are the best.

REFERENCES

[1] ZHANG N, WANG M S, BAN M X, et al. Femtosecond laser drilling 100 μm diameter micro holes with aspect ratios > 20 in a Nickel based superalloy [J]. Journal of Materials Research and Technology-Jmr&T, 2024, 28: 1415-22.

[2] BIERMANN D, KAHLEYSS F, KREBS E, et al. A Study on Micro-Machining Technology for the Machining of NiTi: Five-Axis Micro-Milling and Micro Deep-Hole Drilling [J]. Journal of Materials Engineering and Performance, 2011, 20(4-5): 745-51.

[3] LI Z K, TANG J J, BAI J C. A novel micro-EDM method to improve microhole machining performances using ultrasonic circular vibration (UCV) electrode [J]. International Journal of Mechanical Sciences, 2020, 175.

[4] DAS A K, SAHA P. Machining of circular micro holes by electrochemical micro-machining process [J]. Advances in Manufacturing, 2013, 1(4): 314-9.

[5] ZHANG Z F, WANG W H, JIANG R S, et al. Investigation on geometric precision and surface quality of microholes machined by ultrafast laser [J]. Optics and Laser Technology, 2020, 121.

[6] Marimuthu S, Dunleavey J, Liu Y, et al. Water-jet guided laser drilling of SiC reinforced aluminium metal matrix composites[J]. Journal of Composite Materials, 2019, 53(26-27): 3787-3796.

[7] Li Z, Duan L, Zhao R, et al. Experimental investigation and optimization of modification during coaxial waterjet-assisted femtosecond laser drilling[J]. Optics & Laser Technology, 2024, 177: 111072.

[8] Ren N, Xia K, Yang H, et al. Water-assisted femtosecond laser drilling of alumina ceramics[J]. Ceramics International, 2021, 47(8): 11465-11473.

[9] Krstulović N, Shannon S, Stefanuik R, et al. Underwater-laser drilling of aluminum[J]. The International Journal of Advanced Manufacturing Technology, 2013, 69: 1765-1773.

[10] Laakso M J O, Pagliano S, Shah U, et al. Water in contact with the backside of a silicon substrate enables drilling of high-quality holes through the substrate using ultrashort laser pulses[J]. Optics Express, 2020, 28(2): 1394-1407.

[11] Mendiratta M, Prakash S. Improved quality micro-hole fabrication using backside water assisted laser micro-drilling in titanium[J]. Engineering Research Express, 2025, 7(1): 015402.

[12] Zhang X S, Zhang Z Y, Zhu H, et al. Mass Fabrication of Microholes in Aviation Kerosene Filters Using the Back-water-assisted Picosecond Laser Drilling Technique[J]. Lasers in Engineering (Old City Publishing), 2022, 52.

[13] Wang X, Han B, Ehrhardt M, et al. Optimizing Hole Shape and Improving Surface Quality of Inconel 718 Alloy by High-Temperature Chemical Assisted Laser Processing[J]. Metals and Materials International, 2023, 29(7): 1991-2003.

[14] Li L, Achara C. Chemical assisted laser machining for the minimisation of recast and heat affected zone[J]. CIRP annals, 2004, 53(1): 175-178.